Hindawi
Complexity
Volume 2022, Article ID 9527384, 14 pages
https://doi.org/10.1155/2022/9527384

Research Article

A Novel Hybrid Control Algorithm Sliding Mode-PID for the Active Suspension System with State Multivariable

Duc Ngoc Nguyen and Tuan Anh Nguyen

Automotive Engineering Department, Thuyloi University, 175 Tay Son, Dong Da, Hanoi 100000, Vietnam

Correspondence should be addressed to Duc Ngoc Nguyen; ndn@tlu.edu.vn

Received 25 February 2022; Accepted 19 May 2022; Published 17 June 2022

Academic Editor: Xiaoping Liu

This paper introduces a novel method to control the operation of the active suspension system. In this research, a quarter-dynamic model is used to simulate the vehicle's vibrations. Besides, the sliding mode-PID-integrated algorithm with five state variables is proposed to be used. This is a completely original and novel algorithm. The process of establishing the control algorithm is clearly described. The simulation is performed by the MATLAB software. The results of the paper have shown the advantages of the sliding mode-PID algorithm used in this research. Accordingly, the displacement and acceleration of the sprung mass were significantly reduced when this algorithm was used. The maximum and average values of the displacement of the sprung mass are only 1.31% and 1.29%, respectively, compared with the situation of the vehicle using a passive suspension. Similarly, the value of the acceleration is 6.98% and 2.94%, respectively. In addition, the phenomenon of "chattering" has also been significantly reduced when using this controller. In the future, some more complex algorithms can be proposed.

1. Introduction

The vehicle's vibrations are generated by stimuli from the road surface. These vibrations can affect passengers and cargo on the vehicle. The suspension is used to quell the vehicle's vibrations quickly. The suspension system divides the vehicle into two separate parts, including the sprung mass ms and the un-sprung mass mu [1]. According to [2], the entire vehicle compartment and the sub-assemblies located above the suspension system are called the sprung mass. The remainder is called the un-sprung mass. The excitations will be transmitted from the pavement to the un-sprung mass. It will then continue to be transferred onto the sprung mass through the suspension system. Therefore, the vehicle's vibration can be reduced thanks to the suspension system, which is equipped with the vehicle.

The conventional suspension system used on a vehicle is called a mechanical suspension system (passive suspension system). According to Kashem, a passive suspension system consists of a spring, a shock absorber, and a lever arm [3]. Springs are used to regulate the oscillation. Besides, dampers help to quell the vibrations of the vehicle. For a passive suspension system, the stiffness of the springs and dampers cannot be changed. As a result, the vehicle's smoothness may be affected when the vehicle is on the road. To overcome this situation, several solutions have been proposed to change the stiffness of the suspension system. In [4], Anaya-Martinez et al. suggested the use of a semi-active suspension system. This system uses electromagnetic dampers to replace conventional dampers. According to Sha et al., when an electric current is applied to the shock absorber, the metal particles inside will be tightly arranged. Therefore, the circulation rate of the liquid flow inside will change. This means that the damping stiffness will also change [5]. In addition, changing the spring's stiffness has also been used on some vehicles today [6]. In [7], Sun et al. introduced the air suspension system, which can adjust the stiffness of the air spring. According to Nguyen, the stiffness of the air spring is adjusted based on the air pressure applied to the inside of the balloon. This change is continuous and fully automatic. As a result, the vehicle's smoothness can be further improved [8]. Another method that has been proposed by Fazeli et al. is to

use an active suspension system [9]. The active suspension system has a hydraulic actuator that is placed between the sprung mass and the un-sprung mass. According to Lee et al., the hydraulic actuator operates based on the opening and closing of the servo valves in the system. The operation of the servo valve depends on the supplied voltage signal [10]. The active suspension system can generate an impact force on both the sprung mass and the un-sprung mass. Therefore, the vibration of the vehicle can be improved most effectively.

As for the active suspension system, its most important issue is the control algorithms. The PID controller for active suspension was introduced by Moaaz and Ghazaly [11]. According to them, this controller is determined based on three parameters, including KP, KI, and KD. These parameters can be determined by the self-tuning method. In [12], this method was pointed out by Emam. This is a simple method; however, its accuracy is still not good. Besides, a fuzzy control algorithm is also used to adjust the parameters of the PID controller. This was shown in the study by Ding et al. [13]. Similarly, this method is also mentioned in the paper by Mahmoodabadi and Nejadkourki [14]. The PID controller is only used to control one object. This is the SISO method. Normally, only the value of displacement or acceleration of the sprung mass is considered for this algorithm. It is suitable for a quarter-dynamic model. If more complex models are considered, such as half models or spatial models, MIMO control methods should be used. According to Anh, the LQR controller can control many parameters of the control model [15]. This algorithm is established based on the matrix of the control model [16]. The choice of the coefficients of the matrix is very important. To limit the noise of the system, a Gaussian filter is integrated into this controller [17]. Therefore, the name "LQG controller" was born [18]. The performance of this controller is quite high [19, 20]. However, this is still only a linear control method. In many situations, the system's response is still not stable. Therefore, nonlinear control methods are proposed for using.

Many nonlinear control algorithms have been used for the active suspension system. In [21], Wang et al. introduced the concept of the SMC. According to Chu et al., the SMC helps the active suspension system operate more stably. From there, the phenomenon of rollover can be improved [22]. According to Nguyen, the SMC needs to establish a suitable sliding surface [23]. Controlled objects will move along the sliding surface to move toward a stable position [24]. If the hydraulic actuator is considered in this model, it needs to be linearized appropriately. This has been shown in the study of Bai and Guo [25]. However, these authors only give linear equations without explanation. Therefore, the specific demonstration of the linearization of the actuator for the SM algorithm has been shown in Nguyen's paper [26]. The input signals of the controller can be obtained through a sensor or a camera that is built into the vehicle [27]. According to Azizi and Mobki, the "chattering" phenomenon still exists when using this controller [28]. This phenomenon can be improved by using a hybrid fuzzy SMC; this has been demonstrated by Shaer et al. in [29]. Because the SM control algorithm is a nonlinear method, therefore, the controller design process is extremely complicated [30–33]. Overall, this controller provides stable performance in a wide range of oscillating situations [34–37]. In addition, robust and adaptive control algorithms are also used for the active suspension system. In [38], Yao et al. used the H∞ robust algorithm to improve the efficiency of the suspension system to reduce the roll angle of the vehicle. This algorithm is determined based on the matrix of oscillating states [2]. The system always ensures stability when using this algorithm [39–42]. In some situations, the vehicle's suspension system needs to oscillate continuously to respond well to changes in external stimuli. The adaptive control method is suitable for these situations [43, 44]. Besides, a few nonlinear control algorithms have also been used. Their efficiency is very high [45–47].

In recent years, intelligent control methods have also been studied and widely applied to automotive mechatronic systems. In [48], Haddar et al. used the i-PD algorithm for the active suspension system. In their paper, the MFC method is used. Besides, the PSO algorithms with high performance are also used for the half model to optimize the vehicle's vibration [49]. In many situations, it is difficult to accurately determine the vehicle's vibrational state. Therefore, the use of the fuzzy control algorithm is completely appropriate [50]. According to Khan et al., the membership functions and fuzzy control rules are built based on the experience of the authors [51]. An intermediate state can exist using this algorithm [52–55]. In addition, the use of ANN control algorithms also brings high efficiency to the system [56, 57]. The fundamental oscillation states are stored with the concept of "big data." Based on this data, the controller can self-learn and make judgments in random situations [58–60].

Based on the statements introduced above, this paper focuses on active suspension system control to improve the vehicle's ride comfort and stability. Most of the previous studies used only linear control algorithms to control the active suspension system. Some studies have used the SMC nonlinear control algorithm. However, the "chattering" phenomenon still occurs when using this algorithm. Therefore, this research proposes a method using two integrated control algorithms SMC-PID to limit the "chattering" phenomenon. Besides, the hydraulic actuator is also linearized to establish the five variable models. This is considered the new contribution of the paper. The controller's states that are established in this paper are assumed to be available. For conditions that are not available, the interval observation technique may be used. This is a unique technique [61–63]. The content of this paper consists of four sections. Suspension system issues and literature review are introduced in the first section. In the second section, the vehicle dynamics model and the SMC-PID control algorithm are established. Next, the simulation process will be introduced in the third section. This process is performed in the MATLAB environment. And in the last section, some suggestions are made.

2. Materials and Methods

To simplify the simulation of the vehicle's vibration, a quarter-dynamic model is used in this paper (Figure 1). This model includes the sprung mass ms and the un-sprung mass mu. The link between them is the suspension system, which includes the linear spring and damper. To enhance ride comfort, a hydraulic actuator is fitted alongside the suspension system. Thus, the passive suspension system becomes the active suspension system.

The quarter-dynamics model has two degrees of freedom corresponding to the two directions of motion, including the vertical displacement of the sprung mass z_s and the vertical displacement of the un-sprung mass z_u. Using mechanical theory, the equations describing the oscillations of the vehicle are given as follows:

$$\begin{aligned} m_s\ddot{z}_s &= K(z_u - z_s) + C(\dot{z}_u - \dot{z}_s) + F_A, \\ m_u\ddot{z}_u &= K_T(r - z_u) - K(z_u - z_s) - C(\dot{z}_u - \dot{z}_s) - F_A, \end{aligned} \tag{1}$$

where

K: Stiffness of the spring
C: Stiffness of the damper
K_T: Stiffness of the tire.

To reduce the vehicle's vibration, the hydraulic actuator must generate the impact force F_A. This force acts on both the sprung mass and the un-sprung mass. The impact force F_A is generated based on the pressure change between the two chambers inside the cylinder of the actuator. The value of this force is proportional to the cross-sectional area of the piston (S_p) and the pressure difference (ΔP).

$$F_A = S_p \Delta P. \tag{2}$$

The actuator operates on the voltage signal supplied by the controller. When voltage is applied to the hydraulic actuator, the internal valves move. This displacement changes the fluid pressure inside the cylinder. The relationship between the voltage signal $u(t)$, servo valve displacement x_{sv}, and pressure difference is a very complex multivariable function. It even depends on the displacement of the suspension system x_s. This relationship is shown through equations

$$x_{sv} = \frac{1}{\tau}\int (k_{sv}u(t) - x_{sv})\mathrm{d}t, \tag{3}$$

$$\Delta P = \rho_3 \int \left(x_{sv}\sqrt{P_s - \mathrm{sgn}(x_{sv})\Delta P}\right)\mathrm{d}t - \rho_2 \int \Delta P \mathrm{d}t - \rho_1 S_p \int \dot{x}_s \mathrm{d}t. \tag{4}$$

If the original equations of the hydraulic actuator are used, the design of the SM controller is very difficult. According to Nguyen, the impact force F_A generated by the actuator can be linearized according to equation [26]

$$\dot{F}_A = \xi_1 u(t) - \xi_2 F_A - \xi_3(\dot{z}_s - \dot{z}_u). \tag{5}$$

According to [24], the acceleration of the sprung mass can be approximated as follows:

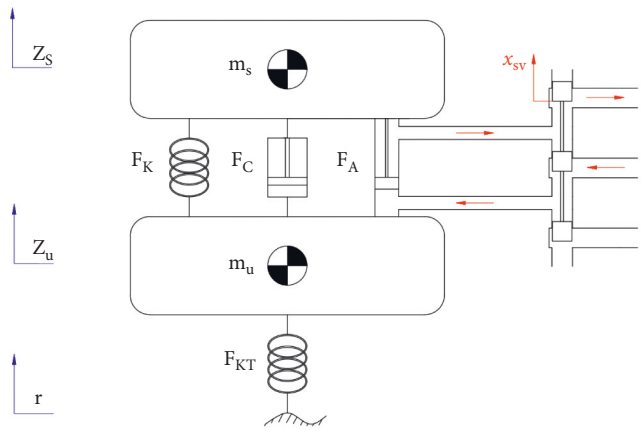

Figure 1: Model of the vehicle dynamics.

$$\ddot{z}_s = \frac{K_T}{\chi m_s}(r - z_u). \tag{6}$$

Let state variables

$$\begin{aligned} x_1 &= z_s, \\ x_2 &= \dot{z}_s, \\ x_3 &= z_u, \\ x_4 &= \dot{z}_u, \\ x_5 &= F_A. \end{aligned} \tag{7}$$

Taking derivatives of state variables,

$$\begin{aligned} \dot{x}_1 &= x_2, \\ \dot{x}_2 &= \frac{1}{m_s}(-Kx_1 - Cx_2 + Kx_3 + Cx_4 + x_5), \\ \dot{x}_3 &= x_4, \\ \dot{x}_4 &= \frac{1}{m_u}(Kx_1 + Cx_2 - (K + K_T)x_3 - Cx_4 - x_5), \\ \dot{x}_5 &= \xi_1 i(t) - \xi_3 x_2 + \xi_3 x_4 - \xi_2 x_5. \end{aligned} \tag{8}$$

Let $e_1(t)$ be the error between the output signal and the set point:

$$e_1(t) = y_s - y. \tag{9}$$

Take the derivative of both sides of equation (9):

$$\begin{aligned} \dot{e}_1(t) &= \dot{y}_s(t) - \dot{y}(t) \\ &= \dot{y}_s(t) - x_2. \end{aligned} \tag{10}$$

Take the second derivative of equation (9):

$$\begin{aligned} \ddot{e}_1(t) &= \ddot{y}_s(t) - \ddot{y}(t) \\ &= \ddot{y}_s(t) - \frac{K_T}{\chi m_s}(x_3 - r). \end{aligned} \tag{11}$$

Take the derivative of both sides of (11), and this is the third derivative of the error $e_1(t)$:

$$\begin{aligned} e_1^{(3)}(t) &= y_s^{(3)}(t) - y^{(3)}(t) \\ &= y_s^{(3)}(t) - \frac{K_T}{\chi m_s}\left(x_4 - \dot{r}\right). \end{aligned} \tag{12}$$

Continuing to derive both sides of (12), the fourth-order differential of the error signal is obtained:

$$\begin{aligned} e_1^{(4)}(t) &= y_s^{(4)}(t) - y^{(4)}(t) \\ &= y_s^{(4)}(t) + \frac{K_T}{\chi m_s m_u}\left(Kx_1 + Cx_2\right. \\ &\quad \left. - \left(K + K_T\right)x_3 - Cx_4 - x_5\right) - \frac{K_T}{\chi m_s}\ddot{r} \end{aligned}. \tag{13}$$

Because the oscillator has five state variables, it is necessary to take the fifth derivative of the output signal $y(t)$:

$$y^{(5)}(t) = \frac{K_T}{\chi m_s m_u}\begin{bmatrix} KC\left(\frac{1}{m_s} + \frac{1}{m_u}\right)x_1 + \left(\frac{C^2}{m_s} + \frac{C^2}{m_u} - K - \xi_3\right)x_2 \\ -C\left(\frac{K}{m_s} + \frac{K + K_T}{m_u}\right)x_3 - \left(\frac{C^2}{m_s} + \frac{C^2}{m_u} - K - K_T - \xi_3\right)x_4 \\ -\left(\frac{C}{m_s} + \frac{C}{m_u} + \xi_2\right)x_5 \end{bmatrix} + \frac{K_T\xi_1}{\chi m_s m_u}i(t) + \frac{K_T}{\chi m_s}r^{(3)}. \tag{14}$$

If $r(t)$ is the disturbance, this value can be ignored. Equation (14) is rewritten as follows:

$$y^{(5)}(t) = \theta_1 x_1 + \theta_2 x_2 + \theta_3 x_3 + \theta_4 x_4 + \theta_5 x_5 + \theta_6 i(t), \tag{15}$$

where

$$\begin{aligned} \theta_1 &= KC\left(\frac{1}{m_s} + \frac{1}{m_u}\right), \\ \theta_2 &= \left(\frac{C^2}{m_s} + \frac{C^2}{m_u} - K - \xi_3\right), \\ \theta_3 &= -C\left(\frac{K}{m_s} + \frac{K + K_T}{m_u}\right), \\ \theta_4 &= -\left(\frac{C^2}{m_s} + \frac{C^2}{m_u} - K - K_T - \xi_3\right), \\ \theta_5 &= -\left(\frac{C}{m_s} + \frac{C}{m_u} + \xi_2\right), \\ \theta_6 &= \frac{K_T\xi_1}{\chi m_s m_u}. \end{aligned} \tag{16}$$

According to the Lyapunov theory, the controlled object will slide along the surface to return to a steady state (Figure 2). Therefore, the slip surface needs to be determined based on the stability condition of the system. The slip surface is a function that depends on the signal of error $e_1(t)$:

$$\sigma = \sum_{i=1}^{n}\sum_{j=0}^{n-1}\alpha_j e_1^{(n-i)}(t). \tag{17}$$

Once the slip surface has been determined, the output signal of the SM controller can be easily determined as equation

$$\begin{aligned} u(t) = \theta_6^{-1}\Bigg[& y_s^{(n)}(t) - \sum_{k=1}^{n}\theta_k x_k(t) + \sum_{i=1}^{n}\sum_{j=0}^{n-1}\alpha_j e_1^{(n-i)}(t) \\ & + Jsgn\left(\sum_{m=0}^{n-1}\sum_{l=0}^{n-1}\alpha_m e_1^{(n-1-l)}(t)\right)\Bigg]. \end{aligned} \tag{18}$$

The output signal of the SM controller is the desired threshold of the subsequent designed PID controller (Figure 3). Let $e_2(t)$ be the error signal of the PID controller:

$$e_2(t) = u(t) - y(t). \tag{19}$$

According to [64], the PID controller includes three stages: a proportional stage, an integral stage, and a derivative stage. For each stage, there is a corresponding coefficient that needs to be selected: K_P, K_I, and K_D. The current signal generated by the PID controller is shown in equation

$$i(t) = K_P e_2(t) + K_I\int_0^t e_2(\tau)\mathrm{d}\tau + K_D\frac{\mathrm{d}e_2(t)}{\mathrm{d}t}. \tag{20}$$

After the controller has been designed, the simulation process is performed. This process happens in the MATLAB environment with specific parameters.

3. Results and Discussion

3.1. Simulation Situations. The results of the research are obtained based on the simulation process. The vehicle parameters used for the calculation are shown in Table 1.

There are three simulation cases used in this paper. In the first two cases, sine pavement excitation is used. However,

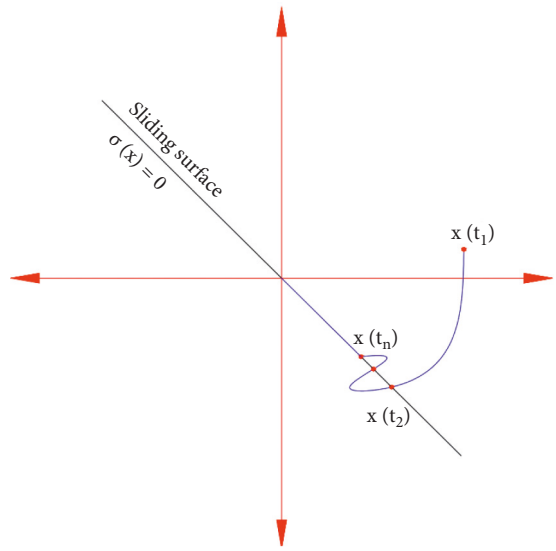

Figure 2: Sliding surface.

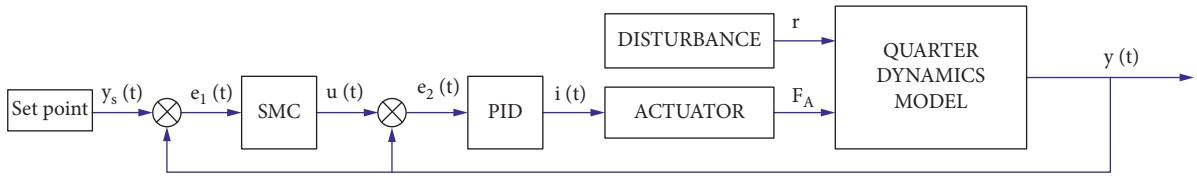

Figure 3: Control system diagram.

Table 1: Parameters of the dynamics model.

Symbol	Description	Value	Unit
m_s	Sprung mass	550	kg
m_u	Un-sprung mass	55	kg
C	Stiffness of the damper	3900	Ns/m
K	Stiffness of the spring	45000	N/m
K_T	Stiffness of the tire	180000	N/m
ξ_1	Coefficient	539561	$N^{3/2}/kg^{1/2}m^{1/2}V$
ξ_2	Coefficient	1	s^{-1}
ξ_3	Coefficient	5512500	N/m

the excitation amplitudes of the oscillations are different. In the third case, the excitation of the pavement is pulse. In each case, the vehicle will be simulated through four situations, including the vehicle using the passive suspension system (none), the active suspension system controlled by a PID controller (PID), the active suspension system controlled by the SM controller (SMC), and the active suspension system controlled by the SMC-PID controller (SMC-PID). The results of the simulation process are analyzed as shown below.

3.2. Results

Case 1. In the first case, the excitation amplitude of the pavement reaches 50 (mm). The displacement of the sprung mass is shown in Figure 4. Accordingly, the maximum value of displacement can be up to 61.96 (mm) if the vehicle uses only the passive suspension system. The displacement of the sprung mass has been markedly reduced when the hydraulic actuator is equipped. Its maximum values are only 23.35 (mm), 7.73 (mm), and 0.81 (mm), respectively. Besides the maximum value, the average value should also be considered. The average value of oscillations calculated according to the RMS criteria of the four situations above reached 32.08 (mm), 12.99 (mm), 3.86 (mm), and 0.42 (mm), respectively. This result shows that the SMC-PID controller helps to reduce displacement of the sprung mass. The vehicle body is almost unchanged during the oscillation.

The change in the acceleration of the sprung mass in the first case is shown in Figure 5. For a conventional mechanical suspension system, the value of the acceleration is the maximum. Its maximum value can be up to 1.29 (m/s^2). After that, this value fluctuates more steadily, with a

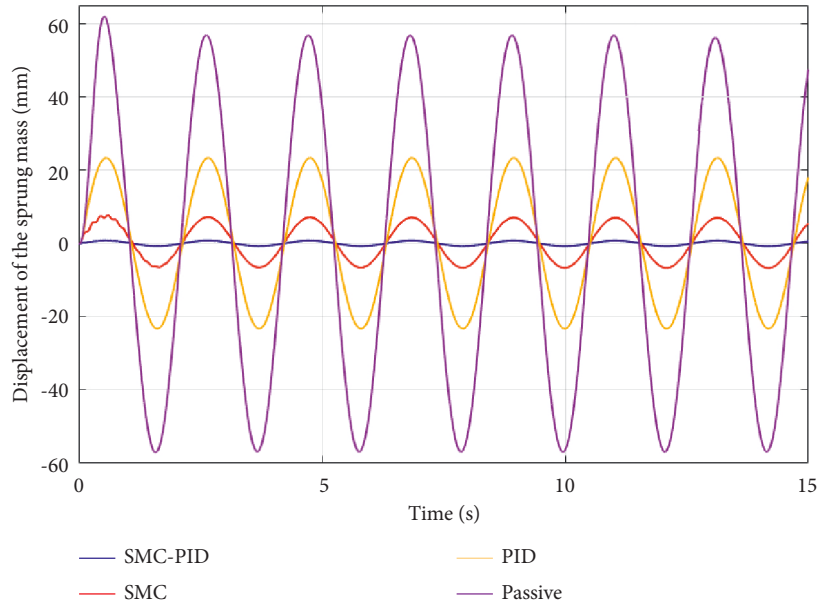

Figure 4: Displacement of the sprung mass (Case 1).

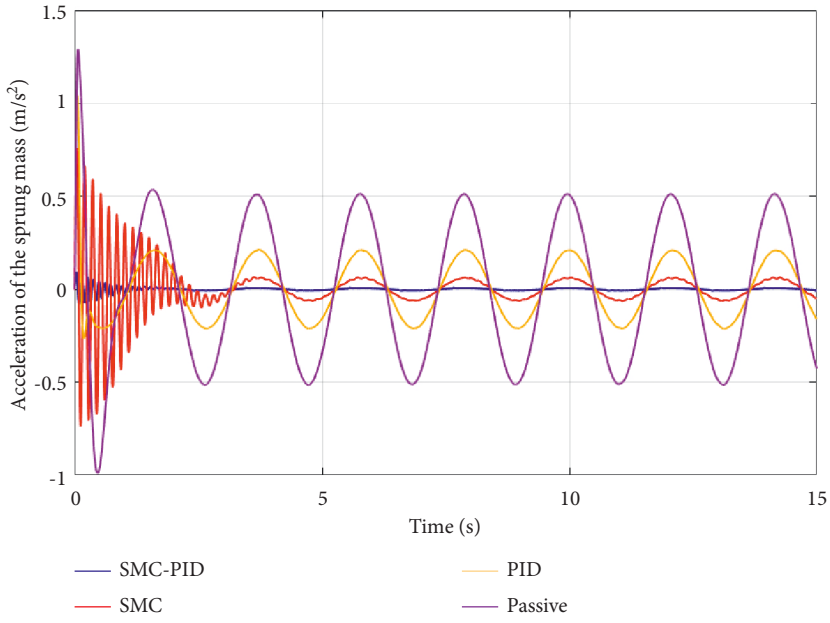

Figure 5: Acceleration of the sprung mass (Case 1).

maximum amplitude of about 0.50 (m/s^2). The average value of the acceleration corresponding to this situation is also the highest, reaching 0.34 (m/s^2).

If the active suspension system is used, the vehicle's vibration can be further improved. According to the results shown in the graph of Figure 5, the maximum value of acceleration when the active suspension system is equipped is 1.04 (m/s^2), 0.76 (m/s^2), and 0.09 (m/s^2), which corresponds to three situations, including PID, SM, and SMC-PID. The average values calculated according to the RMS in the above order are 0.14 (m/s^2), 0.13 (m/s^2), and 0.01 (m/s^2). According to this result, the average value of acceleration when the PID controller and the SMC controller are used is equivalent. In the case of a vehicle using a PID controller, the acceleration takes the form of a pulse in the first phase. From the following phases onward, the acceleration is periodic with time. In contrast, the vehicle's acceleration when using the SMC controller continuously fluctuates. This phenomenon is called "chattering." When using the SMC controller, it is difficult to avoid this phenomenon. However, the SMC-PID integrated controller can solve this problem better. Both the maximum and average values of acceleration when using the SMC-PID controller are very small. In addition, the phenomenon of "chattering" has been significantly

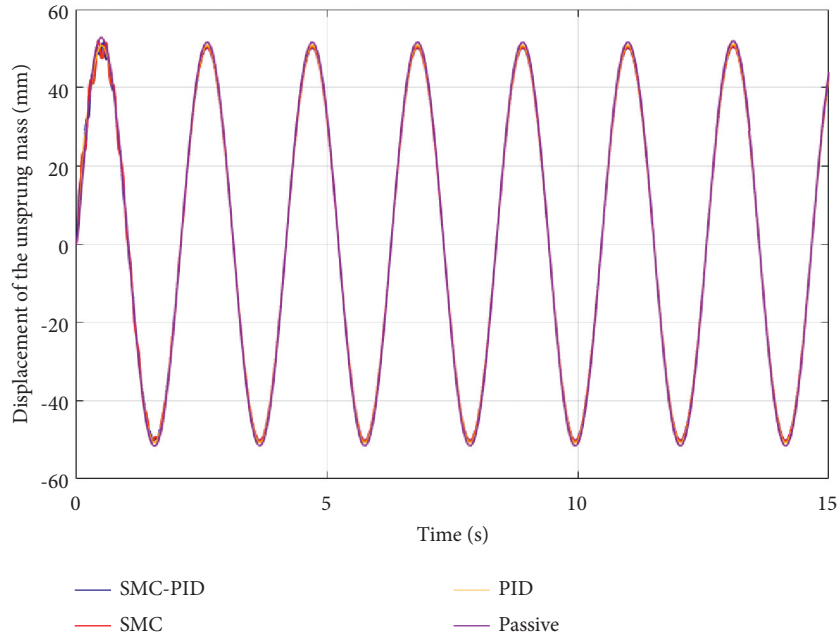

Figure 6: Displacement of the un-sprung mass (Case 1).

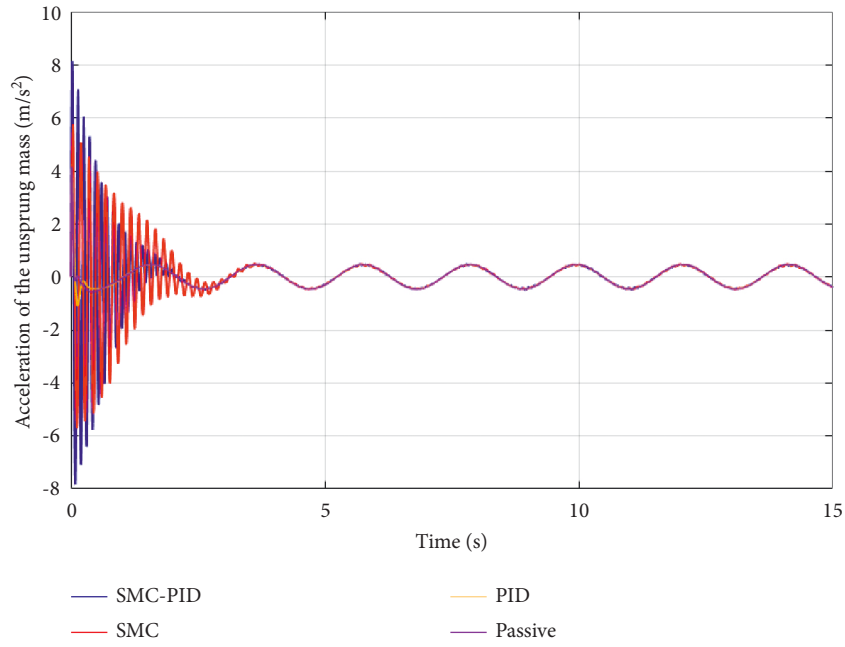

Figure 7: Acceleration of the un-sprung mass (Case 1).

improved. It only appears for a short time when the vehicle starts to oscillate with a rather small amplitude. As a result, the vehicle's smoothness can be enhanced.

For an active suspension system, to reduce displacement and acceleration of the sprung mass, the hydraulic actuator will operate continuously. The impact force generated by the actuator will act on both the sprung mass and the un-sprung mass. The goal of the system is to ensure the stability and comfort of the sprung mass. As a result, the un-sprung mass is likely to fluctuate more. The vibrations of the un-sprung mass influence the overall vibrations of the vehicle. However, this effect is very small. If the oscillation of the un-sprung mass is small, the vehicle's stability and smoothness will be further improved. The changes in displacement and acceleration of the un-sprung mass are shown in Figures 6 and 7.

According to previous results, the displacement of the un-sprung mass is quite large when the vehicle uses the active suspension system [24, 26]. If the displacement of the sprung mass is smaller, the displacement of the un-sprung mass will increase. The same goes for acceleration. However, the SMC-PID controller maintains steady oscillation for the

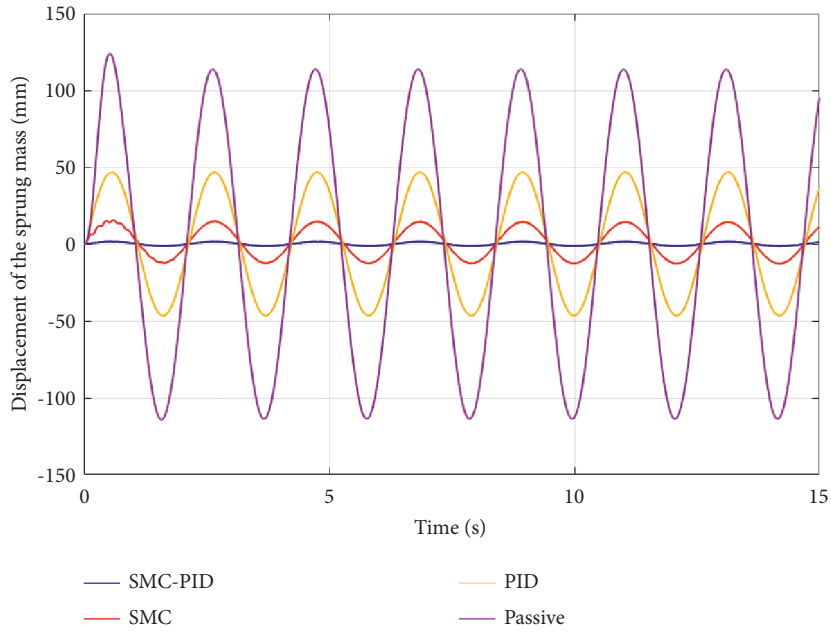

Figure 8: Displacement of the sprung mass (Case 2).

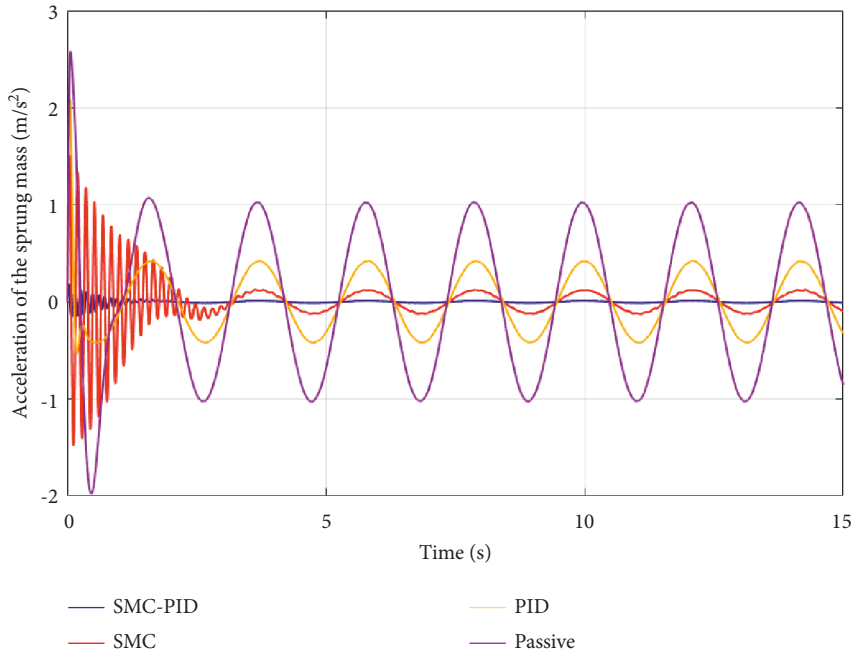

Figure 9: Acceleration of the sprung mass (Case 2).

un-sprung mass. Displacement of un-sprung mass in the case of vehicles with an active suspension system controlled by the SMC-PID method is always closely tracked in the case of vehicles using a conventional passive suspension system. Even though this value is slightly smaller, in the first phase, the acceleration of the un-sprung mass is still quite large. This value rapidly decreases and changes cyclically in subsequent periods. The impact of the first stage is very small. The vibration of the whole vehicle is still guaranteed in the allowed conditions.

Case 2. In the second case, the amplitude of the pavement excitation will be increased. Therefore, the vibration of the vehicle will be greater. This can demonstrate the effectiveness of the active suspension system. In this case, the pavement bump has a magnitude of up to 100 (mm). As a result, the displacement of the sprung mass has increased for the four situations, to 123.92 (mm), 46.70 (mm), 15.60 (mm), and 1.62 (mm), respectively. The average value of displacement also changed accordingly, reaching 78.46 (mm), 31.95 (mm), 9.38 (mm), and 1.01 (mm). The

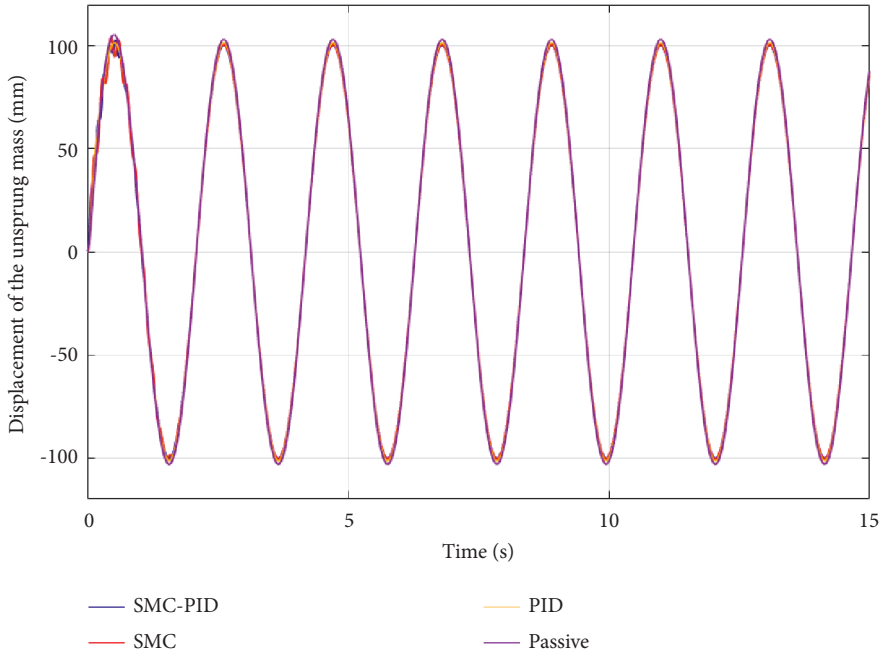

Figure 10: Displacement of the un-sprung mass (Case 2).

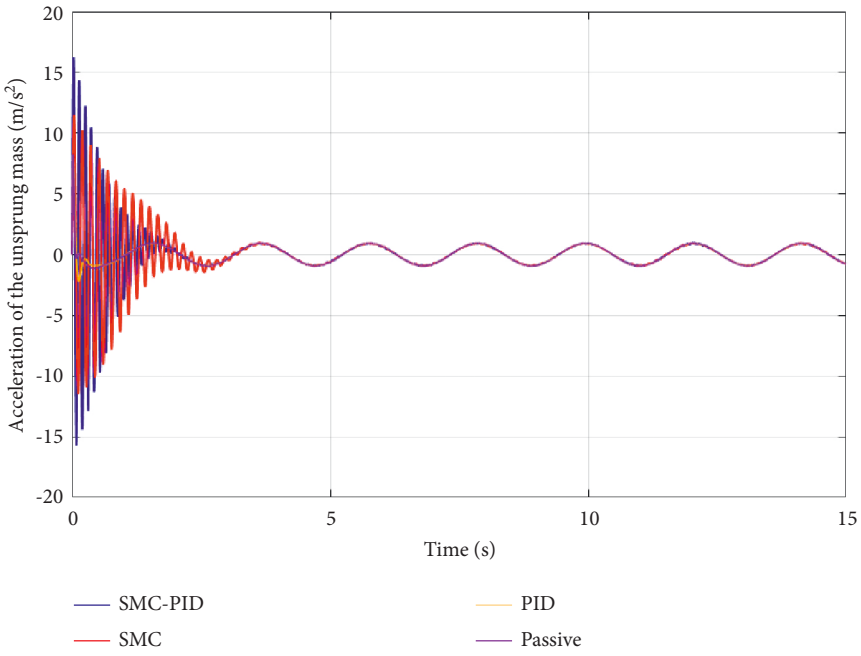

Figure 11: Acceleration of the un-sprung mass (Case 2).

difference in value between the vehicle using the passive suspension system and the vehicle using the active suspension system controlled by the SMC-PID controller can be up to 76.49 times and 77.68 times (Figure 8). This difference is huge. It helps to regulate the vibrational state of the vehicle.

The acceleration of the sprung mass has a great influence on the stability and comfort of the vehicle when traveling on the road. If the value of acceleration is too large, smoothness will no longer be guaranteed. The active suspension system effectively improves this problem. This is demonstrated in Figure 9. According to this result, the acceleration of the sprung mass starts to stabilize in the second phase corresponding to the situation of the vehicle using the passive suspension system and the active suspension system controlled by the PID or SMC-PID algorithm. As for the conventional SMC algorithm, the "chattering" phenomenon still occurs during the whole oscillation process. In particular, the effect of this phenomenon is greatest at the first stage. The maximum values of the acceleration

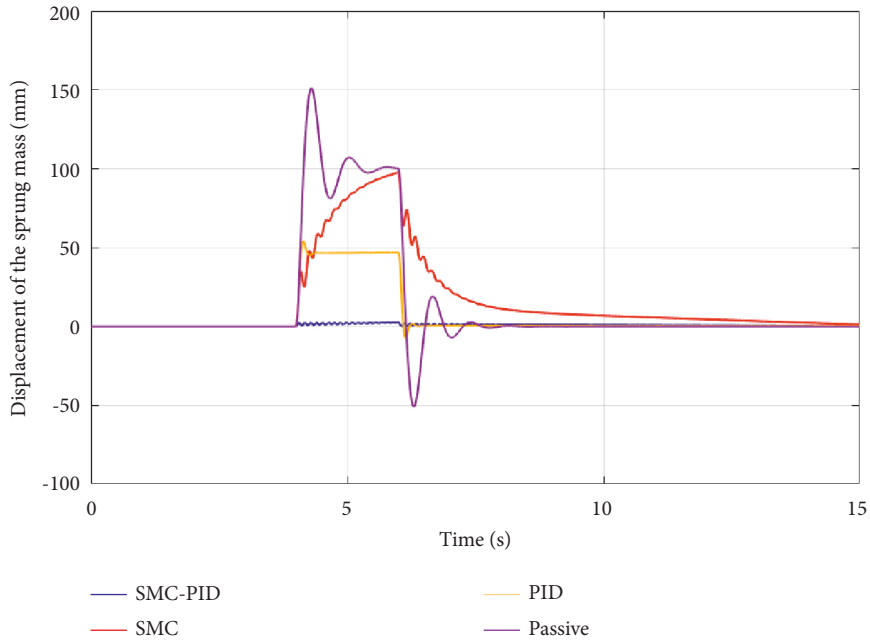

Figure 12: Displacement of the sprung mass (Case 3).

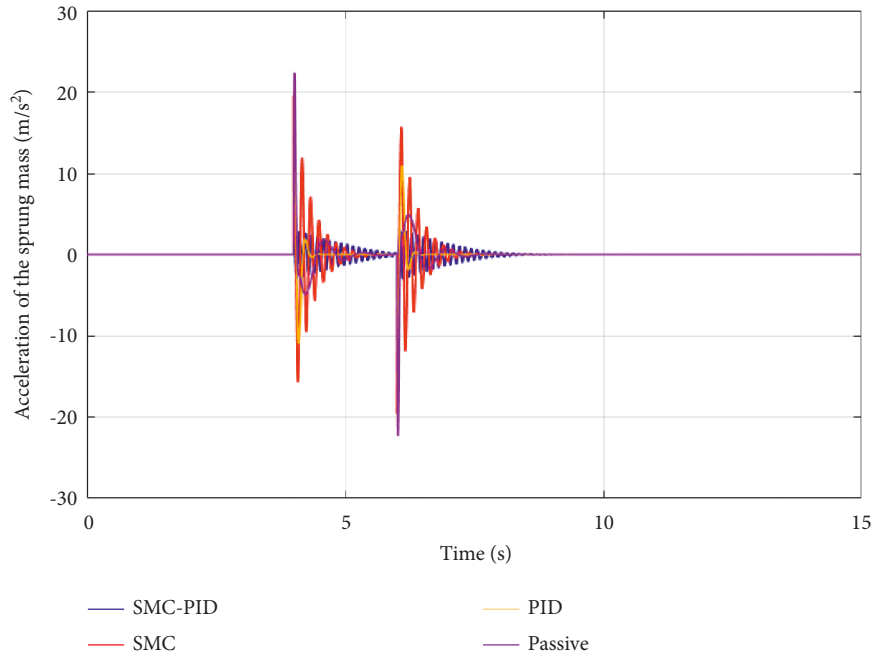

Figure 13: Acceleration of the sprung mass (Case 3).

corresponding to four simulated situations are 2.58 (m/s^2), 2.08 (m/s^2), 1.51 (m/s^2), and 0.18 (m/s^2), respectively. Similarly, their average values have been specifically calculated to be around 0.81 (m/s^2), 0.34 (m/s^2), 0.31 (m/s^2), and 0.03 (m/s^2). The obtained results show that the acceleration of the sprung mass when using the SMC-PID algorithm is only 6.98% and 3.70%, respectively, compared to the situation of the vehicle using the passive suspension system. Again, the efficiency of the control algorithm established in this paper is demonstrated in detail.

Like in the first case, the displacement of the sprung mass in the second case also tended to be closely tracked in all four situations examined (Figure 10). This difference is quite small; it is not more than 2%.

The acceleration of the un-sprung mass has also changed more than in the first case. In subsequent phases of the oscillation, the values of the accelerations are always tracked to each other (Figure 11). In general, the oscillation in the first phase when the vehicle uses the SMC-PID controller does not greatly affect the oscillation of the whole vehicle.

Table 2: The maximum displacement of the sprung mass.

	Passive		PID		SMC		SMC-PID	
	Value (mm)	Percent (%)	Value (mm)	Percent (%)	Value (mm)	Percent (%)	Value (mm)	Percent (%)
Case 1	61.96	100	23.35	37.69	7.73	12.48	0.81	1.31
Case 2	123.92	100	46.70	37.69	15.60	12.59	1.62	1.31
Case 3	150.91	100	54.19	35.91	97.60	64.67	2.51	1.66

Table 3: The average displacement of the sprung mass.

	Passive		PID		SMC		SMC-PID	
	Value (mm)	Percent (%)	Value (mm)	Percent (%)	Value (mm)	Percent (%)	Value (mm)	Percent (%)
Case 1	32.08	100	12.99	40.49	3.86	12.03	0.42	1.31
Case 2	78.46	100	31.95	40.72	9.38	11.96	1.01	1.29

Table 4: The maximum acceleration of the sprung mass.

	Passive		PID		SMC		SMC-PID	
	Value (m/s2)	Percent (%)	Value (m/s2)	Percent (%)	Value (m/s2)	Percent (%)	Value (m/s2)	Percent (%)
Case 1	1.29	100	1.04	81.40	0.76	58.91	0.09	6.98
Case 2	2.58	100	2.08	80.62	1.51	58.53	0.18	6.98
Case 3	22.40	100	21.27	94.96	19.65	87.72	3.22	14.38

Table 5: The average acceleration of the sprung mass.

	Passive		PID		SMC		SMC-PID	
	Value (m/s2)	Percent (%)	Value (m/s2)	Percent (%)	Value (m/s2)	Percent (%)	Value (m/s2)	Percent (%)
Case 1	0.34	100	0.14	41.18	0.13	38.22	0.01	2.94
Case 2	0.81	100	0.34	41.98	0.31	38.27	0.03	3.70

Case 3. For some controllers, even though pavement excitation has ceased, the controller continues to operate. This will cause vehicle instability even though the bumpy road no longer exists. According to Figure 12, the displacement of the sprung mass is greatest when the vehicle uses the passive suspension system. This value can go up to as close as 150.91 (mm). Meanwhile, the displacement of the vehicle body when the SMC-PID algorithm is used is only 2.51 (mm). For the simple SMC controller, the actuator remains active even though the excitation from the pavement has ceased. Even its oscillation is larger than the situation of using a PID controller.

The acceleration of the sprung mass also varies continuously with the excitation conditions of the pavement (Figure 13). The active suspension system controlled by the SMC-PID controller still ensures the stability and smoothness of the vehicle. However, the "chattering" phenomenon persisted for a short period.

The results of the simulation process are summarized in Tables 2–5.

4. Conclusions

Bumps on the road can cause vibrations in the vehicle when traveling on the road. The suspension system is used to quench these oscillations. To improve the stability of the vehicle, an active suspension system is proposed to replace the conventional passive suspension system. This suspension system has a hydraulic actuator, which generates force to act on the sprung mass and un-sprung mass. As a result, the vehicle's smoothness and comfort can be improved. There are several methods used to control the suspension system. Linear control methods such as PID and LQR cannot provide stable performance under many complex conditions. Therefore, the nonlinear control algorithm SMC is used to control the operation of the system. However, the phenomenon of "chattering" still occurs for the SMC algorithm.

This research established a quarter-dynamics model to simulate the vibrations of the vehicle. Besides, the integrated control method SMC-PID is proposed to be used. The simulation is done in the MATLAB environment. There are three types of pavement excitation used for system vibration survey purposes. The outputs of the research include displacements and accelerations of the sprung mass and un-sprung mass. The results of the paper have shown the superiority of the SMC-PID integrated algorithm. Accordingly, the displacement and acceleration of the sprung mass were significantly reduced when this algorithm was used. Compared with other control methods mentioned in the paper, such as PID and SMC, this algorithm provides higher efficiency in all conditions. Besides, the phenomenon of "chattering" has also been significantly reduced. In the future, an experimental process can be conducted to verify the effectiveness of this controller.

Nomenclature

F_A: Force of the hydraulic actuator, N
F_C: Force of the damper, N
F_K: Force of the spring, N
F_{KT}: Force of the tire, N
$i(t)$: Output signal of the PID controller
$r(t)$: Roughness on the road, m
$u(t)$: Output signal of the sliding mode controller
z_s: Displacement of the sprung mass, m
z_u: Displacement of the un-sprung mass, m

Abbreviation

ANN: Artificial neural network
i-PD: Intelligent proportional-derivative
LQG: Linear quadratic Gaussian
LQR: Linear quadratic regulator
MFC: Model-free control
MIMO: Multi-input, multi-output
PID: Proportional-integral-derivative
PSO: Particle swarm optimization
RMS: Root mean square
SISO: Single input, single output
SMC: Sliding mode controller.

Data Availability

The data used to support this research are included within this paper.

Conflicts of Interest

The authors declare that there are no conflicts of interest regarding the publication of this paper.

References

[1] J. Yin, X. Chen, J. Li, and L. Wu, "Investigation of equivalent unsprung mass and nonlinear features of electromagnetic actuated active suspension," *Shock and Vibration*, vol. 2015, Article ID 624712, 8 pages, 2015.

[2] Z.-J. Fu and X.-Y. Dong, "H∞ optimal control of vehicle active suspension systems in two time scales," *Automatika*, vol. 62, no. 2, pp. 284–292, 2021.

[3] S. B. A. Kashem, "A study and review on vehicle suspension system and introduction of a high-bandwidth configured quarter car suspension system," *Australian Journal of Basic and Applied Sciences*, vol. 9, no. 30, pp. 59–66, 2015.

[4] M. Anaya-Martinez, "Control of automotive semi-active MR suspensions for in-wheel electric vehicles," *Applied Sciences*, vol. 10, no. 13, 2020.

[5] S. Sha, Z. Wang, and H. Du, "Research on performance of vehicle semi-active suspension applied magnetorheological damper based on linear quadratic Gaussian control," *Noise & Vibration Worldwide*, vol. 51, no. 7-9, pp. 119–126, 2020.

[6] G. Zepeng, N. Jinrui, L. Lian, and X. Xiaolin, "Research on air suspension control system based on Fuzzy control," *Energy Procedia*, vol. 105, pp. 2653–2659, 2017.

[7] Z. Sun, Y. Shi, N. Wang, J. Zhang, Y. Wang, and S. Xu, "Mechanism and optimization of a novel automobile pneumatic suspension based on dynamic analysis," *Electronics*, vol. 10, no. 18, p. 2232, 2021.

[8] T. A. Nguyen, "Advance the stability of the vehicle by using the pneumatic suspension system integrated with the hydraulic actuator," *Latin American Journal of Solids and Structures*, vol. 18, no. 7, 2021.

[9] S. Fazeli and A. Moarefianpur, "An adaptive approach for vehicle suspension system control in presence of uncertainty and unknown actuator time delay," *Systems Science & Control Engineering*, vol. 9, no. 1, pp. 117–126, 2021.

[10] J. Lee, K. Oh, and K. Yi, "A novel approach to design and control of an active suspension using linear pump control-based hydraulic system," *Proceedings of the Institution of Mechanical Engineers - Part D: Journal of Automobile Engineering*, vol. 234, no. 5, pp. 1224–1248, 2019.

[11] A. O. Moaaz and N. M. Ghazaly, "Fuzzy and PID controlled active suspension system and passive suspension system comparison," *International Journal of Advanced Science and Technology*, vol. 28, no. 16, pp. 1721–1729, 2019.

[12] A. S. Emam, "Fuzzy self tuning of PID controller for active suspension system," *Advances in Powertrains and Automotives*, vol. 1, no. 1, pp. 34–41, 2015.

[13] X. Ding, R. Li, Y. Cheng, Q. Liu, and J. Liu, "Design of and research into a multiple-fuzzy PID suspension control system based on road recognition," *Processes*, vol. 9, no. 12, p. 2190, 2021.

[14] M. J. Mahmoodabadi and N. Nejadkourki, "Optimal Fuzzy adaptive robust PID control for an active suspension system," *Australian Journal of Mechanical Engineering*, pp. 1–11, 2020.

[15] N. T. Anh, "Control an active suspension system by using PID and LQR controller," *International Journal of Mechanical and Production Engineering Research and Development*, vol. 10, no. 3, pp. 7003–7012, 2020.

[16] D. Rodriguez-Guevara, "Active suspension control using an MPC-LQR-LPV controller with attraction sets and quadratic stability conditions," *Mathematics*, vol. 920 pages, 2021.

[17] H. Pang, Y. Chen, J. Chen, and X. Liu, "Design of LQG controller for active suspension without considering road input signals," *Shock and Vibration*, vol. 2017, pp. 1–13, Article ID 6573567, 2017.

[18] R.-x. Xia, J.-h. Li, J. He, D.-f. Shi, and Y. Zhang, "Linear-quadratic-Gaussian controller for truck active suspension based on cargo integrity," *Advances in Mechanical Engineering*, vol. 7, no. 12, 12 pages, Article ID 168781401562032, 2015.

[19] P. Brezas and M. C. Smith, "Linear quadratic optimal and risk-sensitive control for vehicle active suspensions," *IEEE Transactions on Control Systems Technology*, vol. 22, no. 2, pp. 543–556, 2014.

[20] L. Chai and T. Sun, "The design of LQG controller for active suspension based on analytic hierarchy process," *Mathematical Problems in Engineering*, vol. 2010, pp. 1–19, Article ID 701951, 2010.

[21] G. Wang, M. Chadli, and M. V. Basin, "Practical terminal sliding mode control of nonlinear uncertain active suspension systems with adaptive disturbance observer," *IEEE*, vol. 26, no. 2, pp. 789–797, 2021.

[22] D. Chu, X.-Y. Lu, C. Wu, Z. Hu, and M. Zhong, "Smooth sliding mode control for vehicle rollover prevention using active antiroll suspension," *Mathematical Problems in Engineering*, vol. 2015, pp. 1–8, Article ID 478071, 2015.

[23] T. A. Nguyen, "Study on the sliding mode control method for the active suspension system," *International Journal of*

Applied Science & Engineering, vol. 18, no. 5, pp. 1–10, Article ID 2021069, 2021.

[24] T. A. Nguyen, "Advance the efficiency of an active suspension system by the sliding mode control algorithm with five state variables," *IEEE Access*, vol. 9, pp. 164368–164378, 2021.

[25] R. Bai and D. Guo, "Sliding-Mode control of the active suspension system with the dynamics of a hydraulic actuator," *Complexity*, vol. 2018, pp. 1–6, Article ID 5907208, 2018.

[26] D. N. Nguyen, T. A. Nguyen, and N. D. Dang, "A novel sliding mode control algorithm for an active suspension system considering with the hydraulic actuator," *Latin American Journal of Solids and Structures*, vol. 19, no. 1, 2022.

[27] F. Zhao, M. Dong, Y. Qin, L. Gu, and J. Guan, "Adaptive neural-sliding mode control of active suspension system for camera stabilization," *Shock and Vibration*, vol. 2015, pp. 1–8, Article ID 542364, 2015.

[28] A. Azizi and H. Mobki, "Applied Mechatronics: Designing a Sliding Mode Controller for Active Suspension System," *Complexity*, vol. 2021, Article ID 6626842, 2021.

[29] B. Shaer, J.-P. Kenné, C. Kaddissi, and C. Fallaha, "A chattering-free Fuzzy hybrid sliding mode control of an electrohydraulic active suspension," *Transactions of the Institute of Measurement and Control*, vol. 40, no. 1, pp. 222–238, 2016.

[30] D. Wang, D. Zhao, M. Gong, and B. Yang, "Nonlinear predictive sliding mode control for active suspension system," *Shock and Vibration*, vol. 2018, pp. 1–10, Article ID 8194305, 2018.

[31] L. Xiao and Y. Zhu, "Sliding-mode output feedback control for active suspension with nonlinear actuator dynamics," *Journal of Vibration and Control*, vol. 21, no. 14, pp. 2721–2738, 2015.

[32] W. Qin, W. B. Shangguan, and K. Zhao, "A research of sliding mode control method with disturbance observer combining skyhook model for active suspension systems," *Journal of Vibration and Control*, vol. 26, no. 11-12, pp. 952–964, 2020.

[33] J. Sun and K. Zhao, "Adaptive neural Network sliding mode control for active suspension systems with electrohydraulic actuator dynamics," *International Journal of Advanced Robotic Systems*, vol. 17, no. 4, Article ID 172988142094198, 2020.

[34] V. S. Deshpande, P. D. Shendge, and S. B. Phadke, "Active suspension systems for vehicles based on a sliding-mode controller in combination with inertial delay control," *Proceedings of the Institution of Mechanical Engineers - Part D: Journal of Automobile Engineering*, vol. 227, no. 5, pp. 675–690, 2013.

[35] H. Pang, Y. Shang, and P. Wang, "Design of a sliding mode observer-based fault tolerant controller for automobile active suspensions with parameter uncertainties and sensor faults," *IEEE Access*, vol. 8, pp. 186963–186975, 2020.

[36] J. Konieczny, M. Sibielak, and W. Raczka, "Active vehicle suspension with anti-roll system based on advanced sliding mode controller," *Energies*, vol. 13, pp. 5560–21, 2020.

[37] R. J. Lian, "Enhanced adaptive self-organizing Fuzzy sliding-mode controller for active suspension systems," *IEEE Transactions on Industrial Electronics*, vol. 60, no. 3, pp. 958–968, 2013.

[38] J. Yao, M. Wang, and Y. Bai, "Automobile active tilt based on active suspension with H∞ robust control," *Proceedings of the Institution of Mechanical Engineers - Part D: Journal of Automobile Engineering*, vol. 235, no. 5, pp. 1320–1329, 2020.

[39] S. M. Moradi, A. Akbari, and M. Mirzaei, "An offline LMI-based robust model predictive control of vehicle active suspension system with parameter uncertainty," *Transactions of the Institute of Measurement and Control*, vol. 41, no. 6, pp. 1699–1711, 2019.

[40] B. Erol and A. Delibaşı, "Proportional-integral-derivative type H∞ controller for quarter car active suspension system," *Journal of Vibration and Control*, vol. 24, no. 10, pp. 1951–1966, 2018.

[41] W. Li, Z. Xie, P. K. Wong, Y. Cao, X. Hua, and J. Zhao, "Robust nonfragile H∞ optimum control for active suspension systems with time-varying actuator delay," *Journal of Vibration and Control*, vol. 25, no. 18, pp. 2435–2452, 2019.

[42] K. Wang, P. He, J. Tang, and J. Chen, "Static output feedback H∞ control for active suspension system with input delay and parameter uncertainty," *Advances in Mechanical Engineering*, vol. 10, no. 7, 7 pages, Article ID 168781401878658, 2018.

[43] T. C. Nichitelea and M. G. Unguritu, "Design and comparisons of adaptive harmonic control for a quarter-car active suspension," *Proceedings of the Institution of Mechanical Engineers - Part D: Journal of Automobile Engineering*, vol. 236, no. 2-3, pp. 343–352, 2021.

[44] S. Liu, R. Hao, D. Zhao, and Z. Tian, "Adaptive dynamic surface control for active suspension with electro-hydraulic actuator parameter uncertainty and external disturbance," *IEEE Access*, vol. 8, pp. 156645–156653, 2020.

[45] M. Du, D. Zhao, T. Ni, L. Ma, and S. Du, "Output feedback control for active suspension electro-hydraulic actuator systems with a novel sampled-data nonlinear extended state observer," *IEEE Access*, vol. 8, pp. 128741–128756, 2020.

[46] V. S. Deshpande, P. D. Shendge, and S. B. Phadke, "Nonlinear control for dual objective active suspension systems," *IEEE Transactions on Intelligent Transportation Systems*, vol. 18, no. 3, pp. 656–665, 2017.

[47] X. Su, "Master-slave control for active suspension systems with hydraulic actuator dynamics," *IEEE Access*, vol. 5, pp. 3612–3621, 2017.

[48] M. Haddar, R. Chaari, S. C. Baslamisli, F. Chaari, and M. Haddar, "Intelligent PD controller design for active suspension system based on robust model-free control strategy," *Proceedings of the Institution of Mechanical Engineers - Part C: Journal of Mechanical Engineering Science*, vol. 233, no. 14, pp. 4863–4880, 2019.

[49] K. Wu and C. Ren, "Control and stability analysis of double time-delay active suspension based on particle Swarm optimization," *Shock and Vibration*, vol. 2020, pp. 1–12, Article ID 8873701, 2020.

[50] J. Na, Y. Huang, X. Wu, S.-F. Su, and G. Li, "Adaptive finite-time Fuzzy control of nonlinear active suspension systems with input delay," *IEEE Transactions on Cybernetics*, vol. 50, no. 6, pp. 2639–2650, 2020.

[51] M. A. Khan, S. Haroon, E. Ahmad, B. Hayat, and I. Youn, "Active slip control of a vehicle using Fuzzy control and active suspension," *Automatika*, vol. 62, no. 3-4, pp. 386–396, 2021.

[52] H. D. Choi and S. H. You, "Fuzzy finite memory state estimation for electro-hydraulic active suspension systems," *IEEE Access*, vol. 9, pp. 99364–99373, 2021.

[53] P. Swethamarai and P. Lakshmi, "Adaptive-fuzzy fractional order PID controller-based active suspension for vibration control," *IETE Journal of Research*, 2020.

[54] T. A. Nguyen, "Preventing the rollover phenomenon of the vehicle by using the hydraulic stabilizer bar controlled by a two-input Fuzzy controller," *IEEE Access*, vol. 9, pp. 129168–129177, 2021.

[55] T. A. Nguyen, "Improving the Stability of the Passenger Vehicle by Using an Active Stabilizer Bar Controlled by the

Fuzzy Method," *Complexity*, vol. 2021, Article ID 6569298, 2021.

[56] Y. Zhang, Y. Liu, and L. Liu, "Adaptive finite-time NN control for 3-DOF active suspension systems with displacement constraints," *IEEE Access*, vol. 7, pp. 13577–13588, 2019.

[57] S. Bongain and M. Jamett, "Electrohydraulic active suspension fuzzy-neural based control system," *IEEE Latin America Transactions*, vol. 16, no. 9, pp. 2454–2459, 2018.

[58] H. Taghavifar, A. Mardani, C. Hu, and Y. Qin, "Adaptive robust nonlinear active suspension control using an observer-based modified sliding mode interval type-2 Fuzzy neural Network," *IEEE Transactions on Intelligent Vehicles*, vol. 5, no. 1, pp. 53–62, 2020.

[59] Z.-J. Fu, B. Li, X.-B. Ning, and W.-D. Xie, "Online adaptive optimal control of vehicle active suspension systems using single-network approximate dynamic programming," *Mathematical Problems in Engineering*, vol. 2017, pp. 1–9, Article ID 4575926, 2017.

[60] A. Aldair and W. Wang, "A neurofuzzy controller for full vehicle active suspension systems," *Journal of Vibration and Control*, vol. 18, no. 12, pp. 1837–1854, 2011.

[61] A. Khan, W. Xie, B. Zhang, and L.-W. Liu, "A survey of interval observers design methods and implementation for uncertain systems," *Journal of the Franklin Institute*, vol. 358, no. 6, pp. 3077–3126, 2021.

[62] A. Khan, W. Xie, and L.-W. Liu, "Set-membership interval state estimator design using observability matrix for discrete-time switched linear systems," *IEEE Sensors Journal*, vol. 20, no. 11, pp. 6121–6129, 2020.

[63] A. Khan, X. Bai, B. Zhang, and P. Yan, "Interval state estimator design for linear parameter varying (LPV) systems," *IEEE Transactions on Circuits and Systems II: Express Briefs*, vol. 68, no. 8, pp. 2865–2869, 2021.

[64] T. A. Nguyen, "Control the hydraulic stabilizer bar to improve the stability of the vehicle when steering," *Mathematical Modelling of Engineering Problems*, vol. 8, no. 2, pp. 199–206, 2021.